FOLIA HISTOCHEMICA ET CYTOBIOLOGICA
Vol. 48, No. 1, 2010
pp. 71-77

Distributions of PCNA and Cas-3 in rat uterus during early pregnancy

Hakan Öner[1], Jale Öner[1], Ramazan Demir[2]

[1]Department of Histology and Embryology, Faculty of Veterinary Medicine, Mehmet Akif Ersoy University, Burdur, Turkey
[2]Department of Histology and Embryology, Faculty of Medicine, Akdeniz University, Antalya, Turkey

Abstract: The aim of present study was to determine the distributions of proliferating cell nuclear agent (PCNA) and Caspase-3 (Cas-3) and their possible roles in implantation and decidualization during early pregnancy at immunohistochemical level. The tissue samples from pregnant animals between gestational days 1-5 were incubated by PCNA and Cas-3 antibodies and the obtained results were evaluated quantitatively. It was observed that PCNA immunoreactivity in uterine luminal epithelium and glandular epithelium reduced as from day 2 of gestation and disappeared as from day 4 of gestation. PCNA staining intensity in stromal cells and myometrium increased gradually with progressing gestation. While Cas-3 immunoreactivity was strongly detected in luminal and glandular epithelium throughout the whole gestational period, its reactivity markedly increased as from day 3 of gestation. In conclusion, it may suggest that the blastocyst implantation induces the uterine luminal epithelial cell death and stromal cell proliferation around the embryo in the uterus.

Key words: PCNA, Cas-3, early pregnancy, uterine

Introduction

Pregnancy is a complicated process that involves embryo implantation, placentation, embryo development, delivery, etc. In common laboratory rodents the embryo usually attaches to the uterine epithelial lining on days 4-6 of pregnancy and decidualization starts after contact between the basal lamina of the uterine lumen epithelium and the blastocyst [1,2]. Implantation initiates the process of decidualization with proliferation and differentiation of uterine stromal cells into decidual cells in the uterine endometrium surrounding the blastocyst in the antimesometrial zone of the uterus. Then, stromal cells transform toward the mesometrial region from the antimesometrial region to form the decidua basalis, which persists throughout gestation in the antimesometrial region and the decidua capsularis in the mesometrial region [3-5].

During gestation, the uterus undergoes the morphological and physiological changes to accommodate the developing conceptus. These changes that blastocyst attachment and implantation are responsible occur in both epithelial and stromal cells of the uterine endometrium [6-9]. The cell proliferation and apoptosis have an important role among the mechanisms in the attachment and implantation of blastocyst to the uterus endometrium [10-12]. The balance between cell proliferation and death is crucial for successful embryo implantation and maintenance of pregnancy.

At the beginning of pregnancy, the lumen and gland epithelial cell proliferation start firstly in the uterus. Then, the epithelial cell proliferation stops and stromal cell proliferation starts. Progesterone and estrogen hormones secreted by ovarium are responsible for this process [13]. The cell death in the uterine epithelium surrounding the implantation chamber starts at the antimesometrial zone, and as gestation progresses, epithelial degeneration extends to the mesometrial side [8,14,15]. While epithelial cells lining the antimesometrial chamber die when they are in contact with trophoblast cells, epithelial cells lining the mesometrial chamber and the uterine lumen die before the conceptus grows into those regions. Death of these latter epithelial cells is necessary for normal development and function of the chorioallantoic placenta.

There also appear to be differences in the mechanisms of cell death in the two regions, since the cells

Correspondence: H. Öner, Dept. of Histology and Embryology, Faculty of Veterinary Medicine, Mehmet Akif Ersoy University, 15100 Burdur, Turkey; tel. (+90248) 2344500, fax.: (+90248) 2344505, e-mail: hakanoner@mehmetakif.edu.tr, honer23@hotmail.com

Folia Histochem Cytobiol. 2010:48(1): 71 (71-77)
10.2478/v10042-008-0088-2

lining the mesometrial chamber display morphological characteristics of necrotic cells, whereas those lining the antimesometrial chamber appear to be apoptotic [16]. Implantation initiates the process of decidualization with proliferation and differentiation of uterine stromal cells into decidual cells in the uterine endometrium surronding the blastocyst in the antimesometrial zone of the uterus [17]. After the development of the antimesometrial and mesometrial decidua, both regress by apoptosis [4,5,18].

During pre-implantation, the knowledges about the molecular mechanisms underlying uterine apoptosis are still poor. It is suggested that there are two major pathways to activate proteases of the caspase family for apoptosis. The extrinsic pathway involves the death receptors and their ligands. Best studied are the Fas ligands, TNF-α, TGF-β, and their receptors. The intrinsic pathway induces oligomerization of the cytosolic apoptotic protease-activating factor-1 (Apaf-1) and apoptosome formation by cytochrome c release from the mitochondria. The caspase cascade is activated to execute the apoptotic cells in both pathways [19].

The aim of this study is to investigate the distributions of Proliferating Cell Nuclear Antigen (PCNA) and Caspase-3 (Cas-3), that is an apoptosis marker, proteins in rat uterine tissues during early pregnancy.

Material and methods

Experimental Procedures. Mated adult female Wistar albino rats weighing ~190-210 g each (age 12-13 weeks, n=36) were used in this study. The animals were maintained at constant temperature (21±2°C) and humidity (50±5%) on a 12/12 h light/dark cycle (lights on 07.00-19.00). They were housed in plastic cages (six rats per cage) and fed with Standard pellet food and tap water *ad libitium*. The female rats found in estrous were caged overnight together with the male rats (as 2 female/1 male). The next morning the female rats containing sperm in a vaginal smear were designated as gestational day 0. Samples were collected each day from days 1-5 of gestation. The uterus tissue samples of non-pregnant rats found in proestrous were used as control group.

Immunohistochemical procedures. Immunohistochemistry was performed on parafin-embedded sections of the non-pregnant uterus and the developing rat utero-embryonic unit between conception and gestational day 5. Briefly, 1 ml of 1% (v/v) Evans blue (AppliChem, Darmstadt, Germany) in 0.9% (v/v) NaCl was injected into the posterior right femoral vein of 30 impregnated Wistar albino rats under a rompun (5 mg/kg)/ketamin (60 mg/kg) combination anesthesia to identify the implantation areas within the uterus. Ten minutes after the injection the anterior abdominal wall was opened and tissue samples were taken from parts of the uterus containing the dye. The samples were fixed in Bouin's fixative for 6 h, embedded, and then serial sections (5 µm) were collected on slides with poly-L-lysine. After rehydration, samples were transferred to 0.01 M citrate buffer (pH 6.0) and subsequently heated twice in a microwave oven for 5 min each time at 750 W for antigen retrieval. After cooling for 20 min at room temperature, the sections were washed with phosphate-buffered saline (PBS). To remove endogenous peroxidase activity, sections were kept in 3% H_2O_2 for 20 min and then washed with PBS. Sections were incubated with primary mouse-monoclonal PCNA (Dako, Carpinteria, CA) and rabbit-polyclonal Cas-3 (Lab Vision, Fremont, CA) antibodies at 1:100 dilution overnight at 40°C. Negative controls were run routinely in parallel by omitting of the primary antibody. Labeling was visualized using the Universal LSAB kit (Dako, Carpinteria, CA) according to the manufacturer's instructions. Staining was completed with DAB Chromogen (Dako, Carpinteria, CA) for 1-2 min and slides were counterstained with Harris's Hematoxylin, dehydrated, then cover-slipped with permount. All specimens were examined in Nikon-E600 light microscope.

Quantitative evaluation. Sections were evaluated with respect to Cas-3 and PCNA localization in a semiquantitative manner using a light microscope and selected areas were photographed.

HSCORE values of Cas-3 and PCNA staining were obtained in a semiquantitative manner and included both intensity and distribution patterns of staining. Three different fields of five sections per specimen at 400x magnification were evaluated for the analysis of immunohistochemical staining. Values were recorded as percentages of positively stained target cells in each of four intensity categories which were denoted as – (no staining), + (weak), ++ (moderate), +++ (strong). For each tissue, an HSCORE value was derived by summing the percentages of cells that stained at each intensity category and multiplying that value by the weighted intensity of the staining, using the formula HSCORE = $\varepsilon P_i(i + 1)$, where i represents the intensity scores and P_i is the corresponding percentage of the cells [20] .

Statistical analysis. Comparisons of the HSCORE value was performed by the non-parametric Kruskal-Wallis test and subsequent individual comparisons by the Mann-Whitney U test. Results were expressed as mean ±SE. P values less than 0.05 were considered to be statistically significance.

Results

Tissue sections of rat uterus from non-pregnant and days 1-5 of early pregnancy were immunostained to evaluate the distribution of PCNA and Cas-3 proteins. PCNA antibody was used to determine proliferating cells, and Cas-3 antibody was used to determine cells that have capability marker for apoptosis. The semiquantitative and HSCORE values showed PCNA and Cas-3 immunoreactivities were summarized in Table 1 and 2.

PCNA and Cas-3 immunoreactivity were moderately detected in both luminal and glandular epithelium in the uterus tissues of non-pregnant rats (Fig. 1 and 2).

PCNA immunoreactivity was strongly detected in both luminal and glandular epithelium during the first 2 days of gestation (Fig. 3). PCNA expression was observed in stromal cells and myometrium as from day 2 of gestation, and its staining intensity increased gradually with progressing gestation (Fig. 4 and 7). PCNA immunoreactivity was markedly reduced in both luminal and glandular epithelium at day 3 of gestation (Fig. 5) and disappeared as from day 4 of gestation (Fig. 6). PCNA immunoreactivity was strongly expressed in capillary endothelium throughout the whole gestational period. The decidual reaction area was weakly observed at gestational day 4, and the stromal cells in decidual reaction area showed a strong PCNA reac-

Folia Histochem Cytobiol. 2010:48(1): 72 (71-77)
10.2478/v10042-008-0088-2

Table 1. Semiquantitative analysis of PCNA and Cas-3 staining intensities in the groups

Day of gestation	Luminal epithelium	Glandular epithelium	Stromal cells	Capillary endothel	Myometrium	Antibodies
Proestrous	++	++	++	+++	-	PCNA
	++	++	++	+++	++	Caspase-3
1	+++	+++	-	+++	-	PCNA
	+++	+++	+	+++	++	Caspase-3
2	+++	+++	+	+++	+	PCNA
	+++	+++	+	+++	++	Caspase-3
3	+	+	+	+++	+	PCNA
	+++	+++	++	+++	+++	Caspase-3
4	-	-	++	+++	++	PCNA
	+++	+++	++	+++	+++	Caspase-3
5	-	-	+++	+++	++	PCNA
	+++	+++	+++	+++	+++	Caspase-3

Table 2. HSCORE values of PCNA and Cas-3 immunoreactivities at 1-5 day of gestation.

Day of gestation	Luminal epithelium	Glandular epithelium	Stromal cells	Capillary endothel	Myometrium	Antibodies
Proestrous	112,80±9,56^{a}	170±14,22^{a}	76,50±10,02^{a}	400±0,00	-	PCNA
	106,47±10,26^{a}	283,50±12,53^{a}	139,80±11,38^{a}	400±0,00	67,5±7,54^{a}	Cas-3
1	400±0,00^{b}	400±0,00^{b}	-	400±0,00	-	PCNA
	400±0,00^{b}	400±0,00^{b}	17±2,45^{b}	400±0,00	300±0,00^{b}	Caspase-3
2	400±0,00^{b}	400±0,00^{b}	126,40±4,10^{b}	400±0,00	164±4,00^{a}	PCNA
	400±0,00^{b}	400±0,00^{b}	17,5±2,26^{b}	400±0,00	300±0,00^{b}	Caspase-3
3	94,40±13,15^{c}	157,80±7,53^{c}	230,40±35,39^{c}	400±0,00	163,20±2,28^{a}	PCNA
	400±0,00^{b}	400±0,00^{b}	313,33±10,33^{c}	400±0,00	400±0,00^{c}	Caspase-3
4	-	-	360±14,14^{c}	400±0,00	326,40±8,29^{b}	PCNA
	400±0,00^{b}	400±0,00^{b}	313,33±10,33^{c}	400±0,00	400±0,00^{c}	Caspase-3
5	-	-	400±0,00^{d}	400±0,00	368±5,66^{c}	PCNA
	400±0,00^{b}	400±0,00^{b}	400±0,00^{d}	400±0,00	400±0,00^{c}	Caspase-3

$^{a, b, c, d}$ Values in a column with different superscript are significantly different ($p<0,05$)

tion. The rat blastocysts were became visible in the sections at day 5 of gestation. The decidual tissue developing in the antimesometrial side of the uterus was markedly distinguished at this stage. The immunoreactivity of PCNA in the decidual stroma was similar to those of day 4 of gestation (Fig. 8).

Cas-3 imunoreactivity was strongly detected in luminal and glandular epithelium and capillary endothelium throughout the whole gestational period. In stromal cells, while Cas-3 reactivity was weakly expressed during the first 2 days of gestation (Fig. 9), its staining intensity markedly increased as from day 3 of gestation and reached the maximum intensity at day 5 of gestation (Fig. 10). The staining intensity of Cas-3 observed at moderate level in myometrium during the firs 2 days of gestation increased as from day 3 of gestation (Fig. 11 and 12).

Discussion

The uterine responses to implantation involve sequential processes of growth, differentiation, and regression in distinct regions of the uterus, which occur at different time periods [21,22]. The present study was designed to establish a correlation between proliferation and apoptosis in the rat endometrium at immunohistochemical level during early pregnancy. Our immunocytochemistry data showed that Cas-3/PCNA balance in luminal and glandular epithelium shifted toward death inducers as from day 3 of gestation. However, PCNA and Cas-3 expression in stromal cells and myometrium gradually increased with progressing gestation. Zhang and Paria [13] have demonstrated that the number of apoptotic cells determined by TUNEL assay reduced in epithelial cells on day 2 of

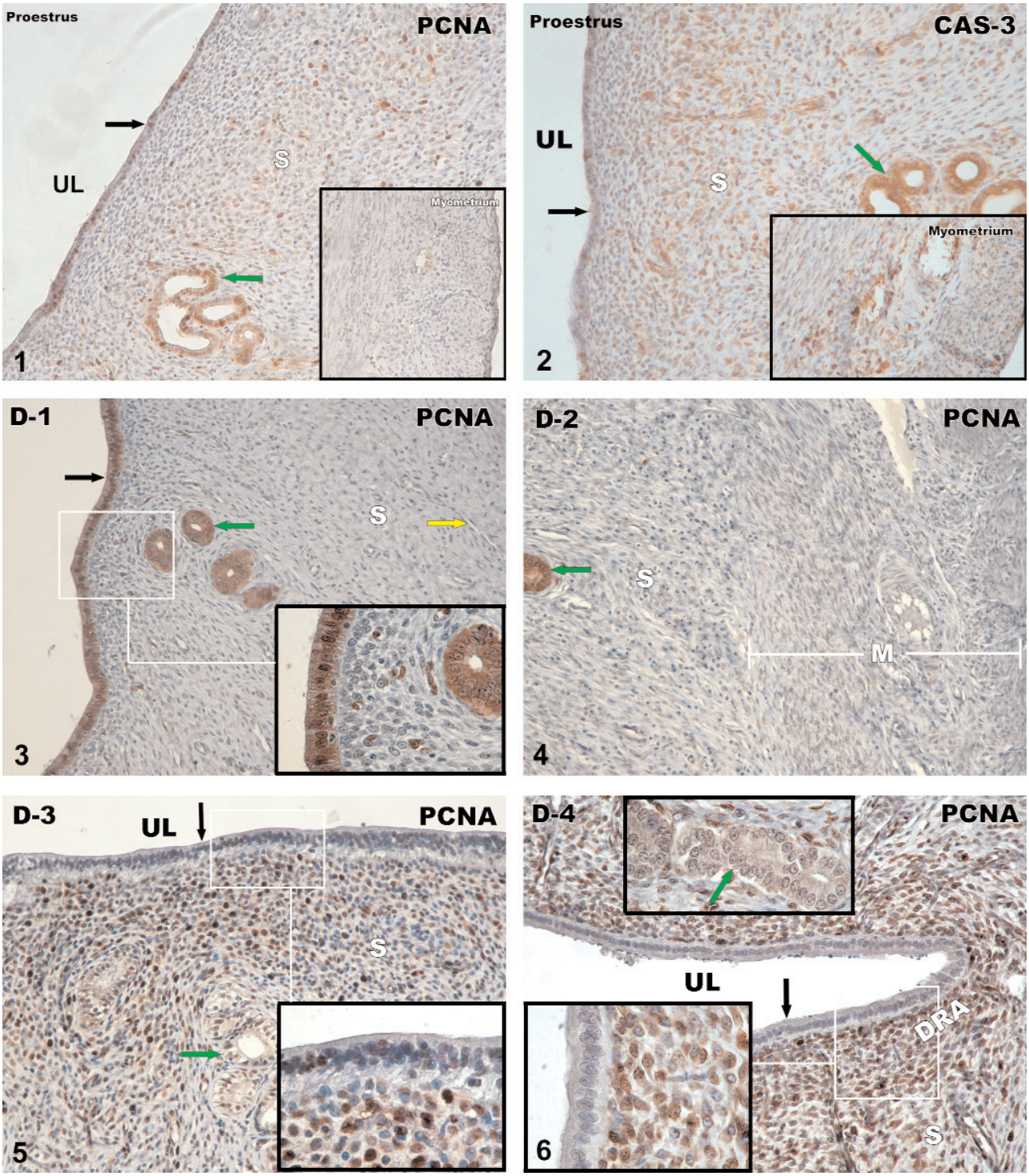

Fig. 1. PCNA immunoreactivity (brown areas) seen in uterine luminal epithelium and stroma of non-pregnant rats. S, stroma; black arrow, uterine luminal epithelium; green arrow, endometrial glands, original magnification ×20. Insert magnification; myometrium ×20. **Fig. 2.** Cas-3 immunoreactivity (brown areas) seen in uterine luminal epithelium and stroma of non-pregnant rats. S, stroma; black arrow, uterine luminal epithelium; green arrow, endometrial glands, original magnification ×20. Insert magnification; myometrium ×20. **Fig. 3.** PCNA immunoreactivity (brown areas) seen in uterine luminal epithelium and stroma at day 1 of gestation. S, stroma; black arrow, uterine luminal epithelium; green arrow, endometrial glands; yellow arrow, capillary, original magnification ×20. Insert magnification ×100. **Fig. 4.** PCNA immunoreactivity (brown areas) seen in stroma (S) and myometrium (M) at day 2 of gestation. green arrows, endometrial glands, original magnification ×20. **Fig. 5.** PCNA immunoreactivity (brown areas) seen in uterine luminal epithelium and stroma at day 3 of gestation. S, stroma; black arrow, uterine luminal epithelium; green arrow, endometrial glands; UL, uterine lumen, original magnification ×20. Insert magnification ×100. **Fig. 6.** PCNA immunoreactivity (brown areas) seen in uterine luminal epithelium and stroma at day 4 of gestation. S, stroma; black arrow, uterine luminal epithelium; green arrow, endometrial glands; UL, uterine lumen; DRA, decidual reaction area original magnification ×40. Insert magnifications ×100.

Folia Histochem Cytobiol. 2010:48(1): 74 (71-77)
10.2478/v10042-008-0088-2

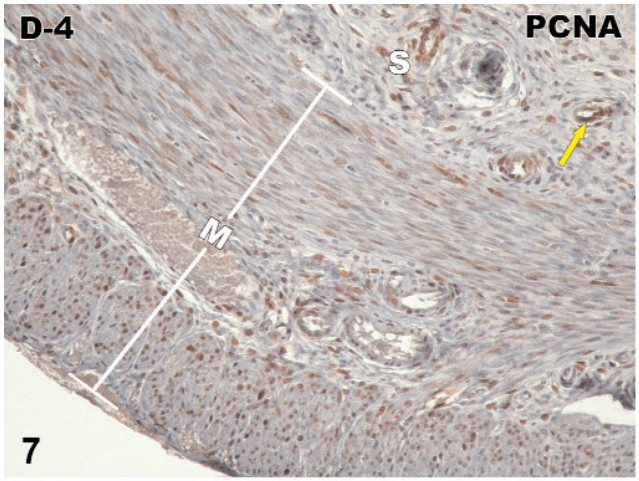

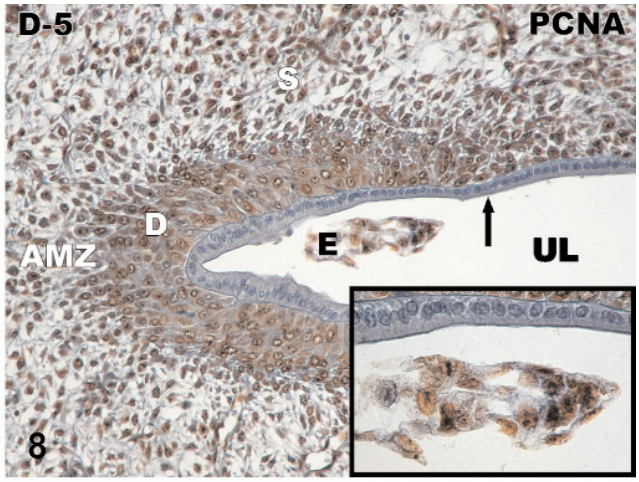

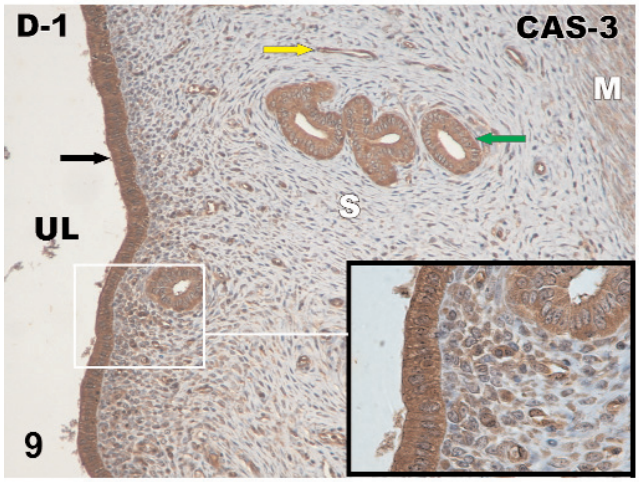

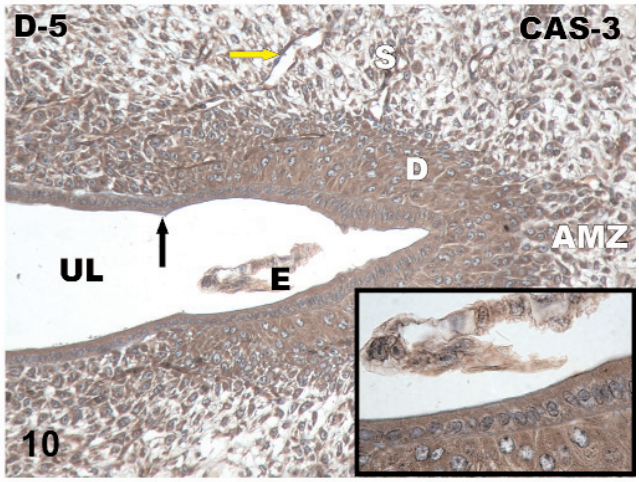

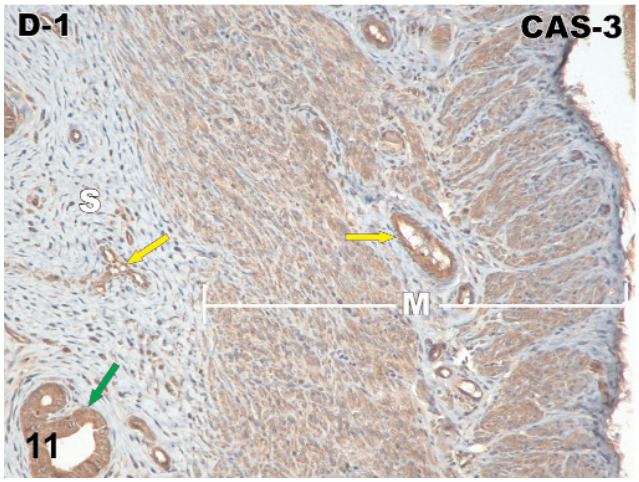

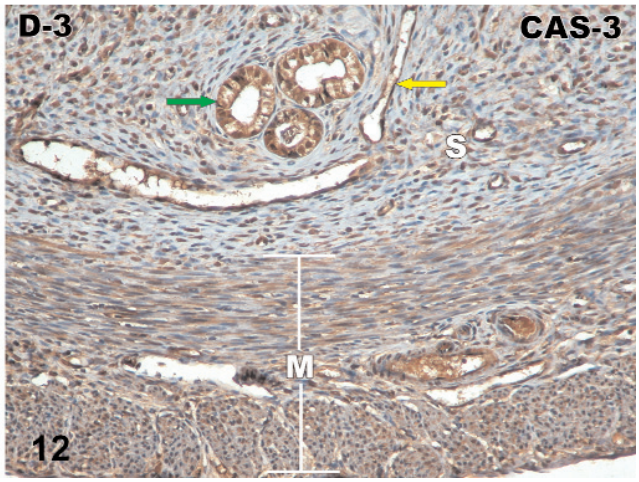

Fig. 7. PCNA immunoreactivity (brown areas) seen in stroma (S) and myometrium (M) at day 4 of gestation, original magnification ×40. **Fig. 8.** PCNA immunoreactivity (brown areas) seen at day 5 of gestation. S, stroma; D, decidua; AMZ, antimesometrial zone; UL, uterine lumen; E, embryo; black arrow, uterine luminal epithelium, original magnification ×40. Insert magnification ×100. **Fig. 9.** Cas-3 immunoreactivity (brown areas) seen in uterine luminal epithelium and stroma at day 1 of gestation. S, stroma; black arrow, uterine luminal epithelium; green arrow, endometrial glands; yellow arrow, capillary; UL, uterine lumen; M, myometrium, original magnification ×20. Insert magnification ×100. **Fig. 10.** Cas-3 immunoreactivity (brown areas) seen at day 5 of gestation. S, stroma; D, decidua; AMZ, antimesometrial zone; UL, uterine lumen; E, embryo; black arrow, uterine luminal epithelium; yellow arrow, capillary, original magnification × 40. Insert magnification ×100. **Fig. 11.** Cas-3 immunoreactivity (brown areas) seen in stroma (S) and myometrium (M) at day 1 of gestation. green arrows, endometrial glands; yellow arrow, capillary original magnification ×20. **Fig. 12.** Cas-3 immunoreactivity (brown areas) seen in stroma (S) and myometrium (M) at day 3 of gestation. green arrows, endometrial glands; yellow arrow, capillary, original magnification ×20.

Folia Histochem Cytobiol. 2010:48(1): 75 (71-77)
10.2478/v10042-008-0088-2

pregnancy after mating in hamsters, and Cas-3 staining was not observed in the epithelial cells on day 2, but some cells in the stroma and muscle layers showed Cas-3 staining. In the mice, they have determined that apoptosis was primarily observed in both the stromal and luminal epithelial layers on day 2 compared with other days of pregnancy (day 1, 3 and 4). Researchers have suggested that a decline in serum estrogen level induces apoptosis. However, they have determined that uterine cell proliferation dramatically increased on day 2 of pregnancy and completely ceased after day 2 of pregnancy. In contrast, they have noticed a significant increase in the number of proliferating cells in the stromal compartment on day 3 and 4 of pregnancy. In another study, uterine cell proliferation during early pregnancy in mice has been previously studied and showed epithelial, but not stromal, cell proliferation on the second day of pregnancy and stromal, but not epithelial, cell proliferation on the third and fourth days of pregnancy [23].

Our findings related to PCNA immunoreactivity decreasing in luminal and glandular epithelium as from day 3 of gestation and increasing in stromal cells as from day 2 of gestation are in accordance with above findings. In contrary, we observed gradually an increase in Cas-3 immunoreactivitiy as well as PCNA immunoreactivitiy in stromal cells with progressing gestation. Both the proliferation and apoptosis processes were happening simultaneously in stromal bed, but the frequency of apoptosis was not similar to the frequency of proliferation during pregnancy. The frequency of proliferation was higher than the frequency of apoptosis. It has been suggested that a higher frequency of cell proliferation may well be related to rapid growth of the uterus and an increase in serum progesterone levels during pregnancy [13].

It has been well documented that the rodent uterine epithelium around the embryo undergoes apoptosis in response to the presence of the blastocyst [5,24,25]. Joswig *et al*. [14]. have observed that the luminal epithelium adjacent to the implantation chamber degenerates with further decidualization, and these regions showed expression of the death receptor TNFR1 and its ligand TNF-α prior to implantation. Due to the localization of the receptor and its ligand in the same cell population, a paracrine or autocrine mechanism has to be taken into account.

Another observation at the present study was an increase at PCNA staining levels in myometrium as from day 2 of gestation while Cas-3 immunoreactivty exists as from day 1 of pregnancy. Cas-3 density is higher than PCNA density through the studied pregnancy process. Some authors have reported that the increased decidual volume and intrauterine pressure can lead to myometrial fibre stretch and muscle layer disintegration, which could account for Cas-3 associated to this mechanical stress, as physical forces activate gen expression and apoptosis in other systems [26-28].

In conclusion, the cell proliferation and cell death occured simultaneously in this study. Cas-3/PCNA rate is in favor of Cas-3 in uterus epithelial cells towards implantation, but in stromal and myometrial cells is in favor of cell proliferation in the rat uterus tissue before implantation. Based on these findings, it may suggest that the blastosist implantation induces the uterine luminal epithelial cell death and stromal cell proliferation around the embryo in the uterus.

References

[1] Abrahamsohn PA, Zorn TMT. Implantation and decidualization in rodents. *J Exp Zool*. 1993;266:603-628.

[2] Demir R. Functional differentiation of the blastocystic ring trophoblast cells in the rat. *Biomed Res*. 1997;8:127-132.

[3] Wang X, Matsumoto H, Zhao X, Das S, Paria BC. Embryonic signals direct the formation of tight junctional permeability barrier in the decidualizing stroma during embryo implantation. *J Cell Sci*. 2004;117:53-62.

[4] Welsh AO, Enders AC. Light and electron microscopic examination of the mature decidual cells of the rat with emphasis on the antimesometrial decidual and its degeneration. *Am J Anat.* 1985;192:215-233.

[5] Welsh AO, Enders AC. Chorioallantoic placenta formation in the rat. I. Luminal epithelial cell death and extracellular matrix modifications in the mesometrial region of implantation chambers. *Am J Anat*. 1991;192:215-231.

[6] Chakraborty C, Gleeson LM, McKinnon T, Lala PK. Regulation of human trophoblast migration and invasiveness. *Can J Physiol Pharmacol* 2002;80:116- 124.

[7] Gu Y, Jow GM, Moulton BC, Lee C, Sensibar JA, Park-Sarge OK, Chen TJ, Giborit G. Apoptosis in decidual tissue regression and reorganization. *Endocrinol.* 1994;135:1272-1279.

[8] O'Shea JD, Kleinfeld RG, Morrow HA. Ultrastructure of decidualization in the pseudopregnant rat. *Am J Anat*. 1983; 166:271-298.

[9] Qin L, Wang YL, Bai SX, Ji SH, Qui W, Tang S, Piao YS. Temporal and spatial expression of integrins and their extracellular matrix ligands at the maternal-fetal interface in the rhesus monkey during pregnancy. *Biol Reprod*. 2003;69:563-571.

[10] Blankenship TN, Enders AC, King BF. Trophopblastic invasion and development of uteroplacental arteries in the macaque. Immunohistochemical localization of cytokeratin, desmin, type IV collagen, laminin and fibronectin. *Cell Tissue Res*. 1993;272:227-236.

[11] Demir R, Kayisli UA, Celik-Ozenci C, Korgun ET, Demir-Weustend AY, Arici A. Structural differentiation of human uterine luminal and glandular epithelium during early pregnancy: an ultrastructural and immunohistochemical study. *Placenta*. 2002;23:672-684.

[12] Kayisli UA, Selam B, Demir R, Arici A. Expression of vasodilatorstimulated phosphoprotein in human placenta: possible implications in trophoblast invasion. *Mol Hum Reprod.* 2002;8:88-94.

[13] Zhang Q, Paria BC. Importance of uterine cell death, renewal, and their hormonal regulation in hamsters that show progesterone-dependent implantation. *Endocrinol*. 2006;147: 2215-2227.

[14] Joswig A, Gabriel HD, Kibschull M, Winterhager E. Apoptosis in uterine epithelium and decidua in response to implan-

tation: evidence for two different pathways. *Reprod Biol Endocrinol.* 2003;1:1-9.
[15] Scott JN, Pendergrass PB. Scanning electron microscopy of the decidual stalk and decidua basalis in the mouse. *Anat Embryo.* 1981;1162:435-441.
[16] Welsh AO, Enders AC. Chorioallantoic placenta formation in the rat. III. granulated cells invade the uterine luminal epithelium at the time of epithelial cell death. *Biol Reprod*. 1993; 49:38-57.
[17] Wang X, Su Y, Deb K, Raposo M, Morrow JD, Reese J, Paria BC. Prostaglandin E2 is a product of induced prostaglandin-endoperoxide synthase 2 and microsomal-type prostaglandin E synthase at the implantation site of the hamster. *J Biol Chem*. 2004;279:30579-30587.
[18] AkcalýKC, Khan SA, Moulton BC. Effect of decidualization on the expression of bax and bcl-2 in the rat uterine endometrium. *Endocrinol*. 1996;137:3123-3130.
[19] Pampfer S, Donnay I. Apoptosis at the time of embryo implantation in the mouse and rat. *Cell Death Differ*. 1999;6: 533-545.
[20] Seval Y, Akkoyunlu G, Demir R, Asar M. Distribution patterns of matrix metalloproteinase (MMP)-2 and -9 and their inhibitors (TIMP-1 and TIMP-2) in the human decidua during early pregnancy. *Acta Histochem.* 2004;106:353-362.
[21] Bell SC. Decidualization: regional differentiation and associated function. *Oxf Rev Reurod Biol*. 1983;5:220-271.
[22] Correia-da-Silva G, Bell SC, Pringle JH, Teixeira NA. Patterns of uterine cellular proliferation and apoptosis in the implantation site of the rat during pregnancy. *Placenta*. 2004; 25:538-547.
[23] Huet-Hudson YM, Andrews GK, Dey SK. Cell type-specific localization of *c-myc* protein in the mouse uterus: modulation by steroid hormones and analysis of the periimplantation period. *Endocrinology.* 1989;125:1683-1690.
[24] Parr EL, Tung HN, Parr MB. Apoptosis as the mode of uterine epithelial cell death during embryo implantation in mice and rats. *Biol Reprod.* 1987;36:211-225.
[25] Schlafke S, Welsh AO, Enders AC. Penetration of the basal lamina of the uterine luminal epithelium during implantation in the rat. *Anat Rec*. 1985;212:47-56.
[26] Leri A, Claudio PP, Li Q, Wang X, Reis K, Wang S, Malhotra A, Kajstura J, Anversa P. Stretchmediated release of angiotensin II induces myocyte apoptosis by activating p53 that enhances the local renineangiotensin system and decreases the Bcl-2-to-Bax protein ratio in the cell. *J Clin Invest*. 1998;101:1326-1142.
[27] Miyashita T, Ree J. Tumor suppressor p53 is a direct transcriptional activactor of the human bax gene. *Cell*. 1995;80: 293-299.
[28] Shynlova OP, Oldenhof AD, Liu M, Langille L, Lye SJ. Regulation of cfos expression by static stretch in rat myometrial smooth muscle cells. *Am J Obstet Gynecol*. 2002;186:1358-1365.

Submitted: 1 July, 2009
Accepted after reviews: 19 October, 2009